Paramagnetic neutron scattering from Pd_2MnSn

H. A. Graf*
Hahn-Meitner Institut, D-1000 Berlin 39, Federal Republic of Germany

P. Böni† and G. Shirane
Physics Department, Brookhaven National Laboratory, Upton, New York 11973

M. Kohgi and Y. Endoh
Physics Department, Tohoku University, Sendai 980, Japan
(Received 21 February 1989)

Paramagnetic neutron scattering spectra from the localized ferromagnet Pd_2MnSn have been reexamined at $T=210$ K ($1.1T_C$), primarily at large-q values. The measured profiles are compared with theoretical profiles calculated according to the three-pole approximation theory from the magnetic exchange constants up to the sixth-nearest-neighbor shell. The calculated linewidths agree reasonably with the observed widths, but not the line shapes; the data show no indication of side peaks at finite energy, as predicted by the theory for the higher-q values. The measurements can be fitted well, however, by a parametrized spectral weight function based on the three-pole approximation.

I. INTRODUCTION

The Heusler compound Pd_2MnSn is a localized metallic ferromagnet with a Curie temperature of $T_C=193$ K. It has a cubic structure, space group $Fm3m$, with a lattice constant $a=6.38$ Å. The magnetic behavior below T_C is well understood. It was shown by Noda and Ishikawa[1,2] that the spin-wave dispersion relations can be described by the Heisenberg model, if at least six exchange interaction parameters are taken into account. In contrast to this, a thorough theoretical understanding of the paramagnetic scattering above T_C is still lacking, primarily because of the metallic nature of this Heusler compound.

The usual starting point for interpreting the neutron experiments above T_C is the scattering function

$$S(q,\omega)=2k_BT\chi(0)\frac{\kappa_1^2}{\kappa_1^2+q^2}F(q,\omega)\frac{\hbar\omega/k_BT}{1-\exp(-\hbar\omega/k_BT)}\ . \tag{1}$$

Here $\chi(0)$ is the bulk (dc) susceptibility, κ_1 the inverse correlation length, $F(q,\omega)$ the spectral weight function, and the last term in Eq. (1) contains the detailed balance factor. While this general form of $S(q,\omega)$ is commonly accepted, the particular function $F(q,\omega)$, that has to be used for describing the paramagnetic scattering in Pd_2MnSn over a wide q range, is not clear. A spectral weight function derived from the asymptotic renormalization-group theory[3,4] has very successfully been applied to the interpretation of the paramagnetic scattering in Ni (Ref. 5) and EuO.[6] There is no question, that this theory should also be applicable to Pd_2MnSn, as long as the dynamical scaling assumptions are fulfilled; in the small-q range, and at temperatures close to T_C, where the linewidth Γ can be expressed as $\Gamma=Aq^{2.5}$. Dipolar interactions, which also lead to a breakdown of dynamical scaling,[7,8] should only be important at very small-q values (see Sec. III). The implications of dipolar effects on the critical dynamics of ferromagnets have recently been taken into account by a theoretical approach based on the mode-coupling theory.[9,10]

We have reexamined the paramagnetic scattering in Pd_2MnSn close to T_C ($T=1.1T_C$) primarily at large-q values, where the theoretical concepts for describing the spin dynamics are not evident. Shirane *et al.*[11] have fitted the neutron scattering data measured at $1.1T_C$ over a wide q range, with a pure Lorentzian as spectral weight function. Introducing a heuristic expression for the q dependence of the linewidth Γ, they were able to describe the paramagnetic scattering in the whole Q,ω space by only two parameters. Kohgi *et al.*[12] have analyzed their data, which were mainly collected at higher temperatures up to $4T_C$, by using the result of the three-pole approximation theory.[13,14] For small-q values, the weight function based on the three-pole approximation is similar to a Lorentzian, at larger-q values it develops a side peak at finite energy. High-resolution data are necessary to make such a structure visible in the measurement. Böni and Shirane,[15] however, have conjectured, that the long-range nature of the exchange interactions should rather lead to a singly peaked profile (peak at $E=0$), since possible excitations at finite energy will be smeared out.

It was the objective of the present work, to clarify the validity of the three-pole approximation for describing the paramagnetic scattering in Pd_2MnSn at q values up to the zone boundary. Since the only parameters occurring in this theory, δ_1 and δ_2, can be derived from known magnetic exchange constants J_i, the theory is basically parameter free. A computer program was written to calculate δ_1 and δ_2 from the exchange constants given in

Ref. 1 up to the sixth-nearest-neighbor shell, and the results of these calculations are compared with the measurements and with fits to the data, where the three-pole approximation was used as a model function only, treating δ_1 and δ_2 as free variables.

II. EXPERIMENT

The single crystal used in the present experiments was the same as that investigated by Shirane *et al.*[11] and Kohgi *et al.*[12] It has a volume of about 3 cm^3 and a mosaic spread of about 0.8°. The experiments were performed on triple-axis spectrometers at the Brookhaven High-Flux Beam Reactor. The spectrometers were operated in the "constant-Q" mode, with the final energy fixed at 14.7 meV, and a pyrolytic graphite filter inserted in front of the detector for eliminating the higher-order neutrons. The crystal was mounted in a cryostat with $[1\bar{1}0]$ perpendicular, and the paramagnetic scattering was measured at points $(1+\zeta,1+\zeta,1+\zeta)$ of the reciprocal lattice. The vertical collimations were approximately 50'-115'-150'-240', and were similar for all experiments.

High-resolution data were collected using an unpolarized beam setup with horizontal collimations 20'-20'-20'-40'. Figure 1 shows an example for the raw data obtained by this configuration at $\zeta=0.35$. The open dots denote the paramagnetic scattering measured at 210 K. The solid dots correspond to a measurement in the ferromagnetic phase at 78 K, which was performed in order to determine the background for the paramagnetic scattering. Below T_C, a broad spin-wave peak is well separated from the strong peak at zero energy, which is mainly due to incoherent nuclear scattering. The width of this incoherent peak, FWHM=0.55 meV below and above T_C, corresponds to the instrumental resolution. The data point at $E=10$ meV below and above T_c was contaminated with some weak extra nuclear scattering, which was corrected for. The solid line shown in Fig. 1 is a Gaussian fit to the spin-wave peak including the instrumental resolution, with another Gaussian added for the incoherent peak. The shift of the intensity maximum in the paramagnetic scattering towards positive energy transfer is mainly due to the higher-order contaminants in the incoming neutron beam, which are also counted by the monitor and, thus, lead to measuring times, which are relatively too short for the small incident energies. This effect of higher-order wavelengths on the monitor can be seen from a comparison with Fig. 2, where the paramagnetic scattering for $\zeta=0.15$, 0.35, and 0.46 is shown together with theoretical curves discussed in Sec. III. The data points plotted as solid dots represent basically the

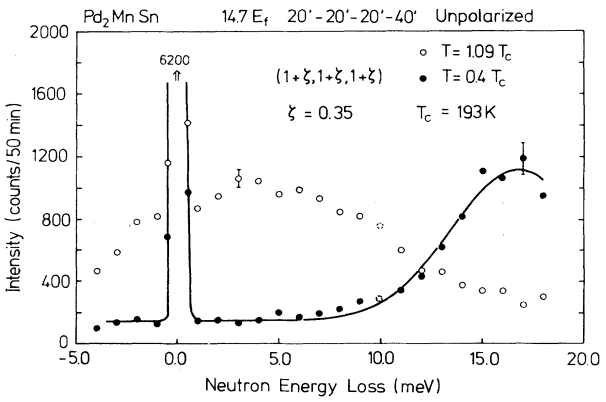

FIG. 1. Constant-Q scans at $\zeta=0.35$ using a high-resolution unpolarized beam setup. The open dots and the solid dots represent raw data measured at $T=1.09T_C$ and $T=0.4T_C$, respectively. The solid line is a Gaussian fit to the magnon peak including the instrumental resolution, with another Gaussian added for describing the incoherent peak at $E=0$ meV. The data point at $E=10$ meV was corrected for some weak extra nuclear scattering. The shift of the intensity maximum in the paramagnetic scattering towards higher energies is mainly due to the effect of higher-order wavelengths on the neutron beam monitor, as discussed in the text.

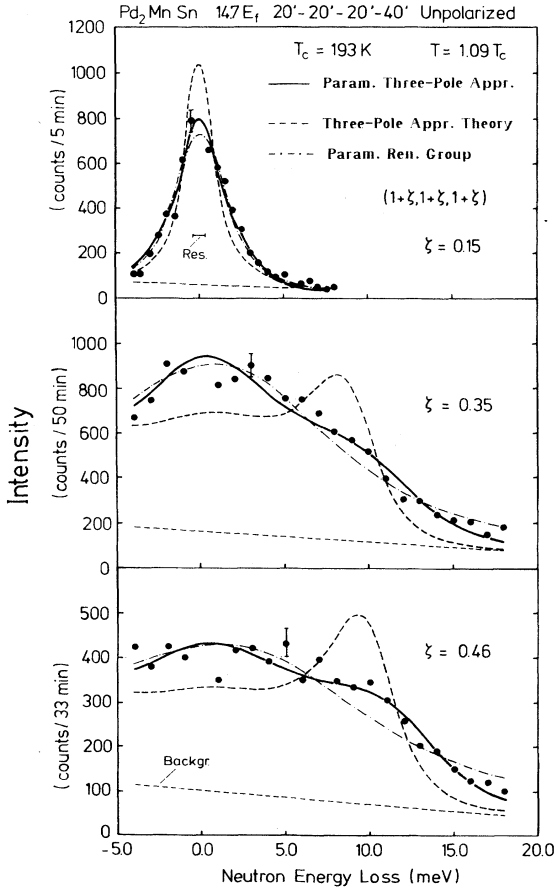

FIG. 2. Constant-Q scans at $\zeta=0.15$, 0.35, and 0.46, and $T=1.09T_C$, using the high-resolution unpolarized beam setup. The experimental data (solid dots) are corrected for the effect of higher-order wavelengths on the neutron beam monitor. The linear background assumed in the fitting procedure is indicated by the inclined short-dashed line. The solid line is a fit based on the three-pole approximation with δ_1 and δ_2 as free parameters, while the dashed line represents the three-pole approximation theory without adjustable parameters, except for a scale factor. The dot-dashed line is a fit with the modified renormalization-group theory.

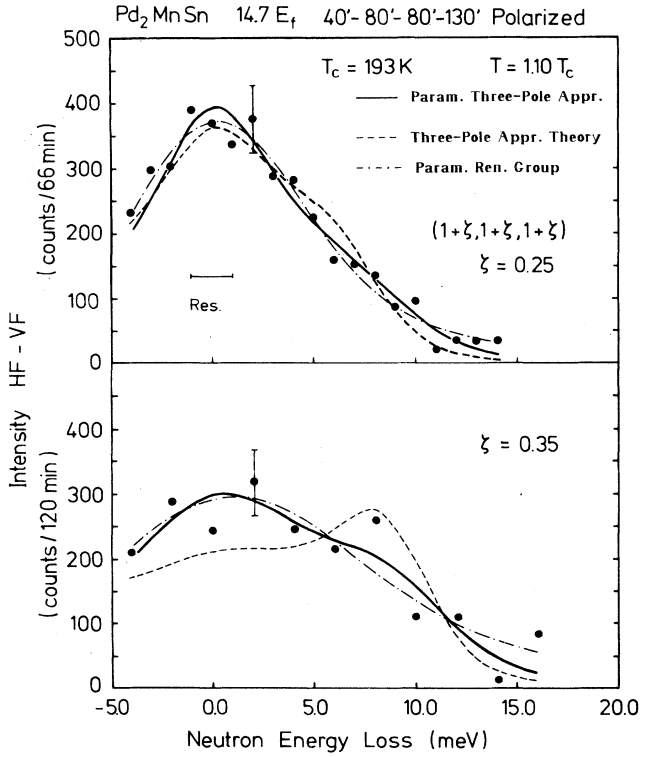

FIG. 3. Constant-Q scans at $\zeta=0.25$, 0.35, and $T=1.10T_C$, using a polarized beam setup. The experimental data (solid dots) represent the difference between measurements made with a horizontal and a vertical field, respectively, applied at the sample position. The data are corrected for the effect of higher-order wavelengths on the neutron beam monitor. The solid line is a fit based on the three-pole approximation with δ_1 and δ_2 as free parameters, while the dashed line represents the three-pole approximation theory without adjustable parameters, except for a scale factor. The dot-dashed line is a fit with the modified renormalization-group theory.

raw intensities, except that they are corrected for the effect of higher-order contaminants, as described in Ref. 16. The thermal factors, which also increase the intensities at higher-energy transfer, are contained in Eq. (1), and were applied to the calculated curves. For comparison with the theory, a linear background indicated by the short-dashed line was assumed, whose inclination just reflects the correction for higher-order wavelengths. The background was taken from the flat part between spin wave and incoherent peak in the corresponding 78 K measurements, after scaling with the factor 0.9, which allows for the different absorption at 78 K compared to 210 K. This absorption factor was determined by transmission measurements. For the fitting procedures discussed in the next session, the data point at $E=0$ meV was omitted, since the sharp incoherent peaks above and below T_C could not be reliably subtracted from one another.

In order to avoid any ambiguities in separating the magnetic from the nuclear scattering, additional measurements were made with a polarized beam setup, where the pure magnetic signal is obtained by the difference technique.[11] The data shown in Fig. 3 correspond to the difference of the intensities measured with a horizontal field along the scattering vector and a vertical field, respectively, applied at the sample, while a spin-flipper device is in operation. The only correction necessary arises from the effect of the higher-order wavelengths on the beam monitor. Heusler crystals were used as monochromator and analyzer in the triple-axis spectrometer, which was again operated in the constant-Q mode with the final energy fixed at 14.7 meV and a graphite filter in front of the detector. In order to obtain enough intensity, the horizontal collimation had to be very relaxed. It was 40'-80'-80'-130' for the scans shown in Fig. 3.

III. RESULTS AND DISCUSSION

The paramagnetic scattering has primarily been analyzed by applying the three-pole (TP) approximation theory.[13,14] The following expression was used as the spectral weight function in Eq. (1):

$$F_{\mathrm{TP}}(q,\omega)=\frac{1}{\pi}\frac{\tau\delta_1\delta_2}{\omega^2\tau^2(\omega^2-\delta_1-\delta_2)^2+(\omega^2-\delta_1)^2} . \quad (2)$$

The parameters δ_1 and δ_2 are related to the second and fourth moments, $\langle\omega^2\rangle$ and $\langle\omega^4\rangle$, of $F_{\mathrm{TP}}(q,\omega)$ by $\delta_1=\langle\omega^2\rangle$ and $\delta_1\delta_2=\langle(\omega^2-\langle\omega^2\rangle)^2\rangle$ and τ is approximated by

$$\tau=\sqrt{2/(\pi\delta_2)} . \quad (3)$$

For a given geometrical spin arrangement δ_1 and δ_2 are solely determined by the wave vector, the temperature, the spin S, and the exchange constants J_i of the magnetic system. In the case of EuO and EuS, where only nearest- and next-nearest neighbors, i.e., J_1 and J_2, are important, values of δ_1 and δ_2 for finite temperatures have been calculated by Young and Shastry.[14] Using and extending their algorithms, a computer program was written, which allows us to evaluate δ_1 and δ_2 for a long-ranged magnetic system, such as Pd_2MnSn, by including contributions from exchange interactions up to the sixth-nearest-neighbor shell. The results of such calculations for the [111] direction in Pd_2MnSn are summarized in Table I. The calculations were made for the reduced temperatures at which the experiments were performed, i.e., $T=1.10T_C^{\mathrm{calc}}$ and $T=1.09T_C^{\mathrm{calc}}$, T_C^{calc} is the phase transition temperature calculated within the framework of the three-pole approximation theory. It is 175.3 K and thus substantially lower than the experimentally observed T_C of 193 K, while in the case of EuO and EuS calculated and observed transition temperatures are in close agreement. The discrepancy indicates, that either the parameter set used or the theory does not perfectly describe the paramagnetic scattering in Pd_2MnSn. The numerical values for the exchange constants J_1 to J_6, employed in the calculations, were taken from Ref. 1, and are also listed in Table I. For consistency, the same value $S=2.1$, for which the exchange constants had been derived, was used as spin S.

In Fig. 4 $F_{\mathrm{TP}}(q,\omega)$, which is symmetrical in ω, is plot-

TABLE I. δ_1, δ_2, and Γ values calculated by the three-pole approximation theory for $T=1.10T_C^{\text{calc}}$ with $T_C^{\text{calc}}=175.3$ K, using the exchange constants up to the sixth-nearest-neighbor shell from Ref. 1. The values in parentheses represent calculations for $T=1.09T_C^{\text{calc}}$. Bottom table shows exchange constants in units of meV from Ref. 1 used in the calculations (spin $S=2.10$).

ζ	δ_1 (meV)^2	δ_2 (meV)^2	Γ (meV)
0.05	0.11	33.48	0.02
0.10	1.04	36.81	0.22
0.15	4.30	42.02	0.88
	(4.34)	(42.09)	(0.89)
0.20	11.26	48.89	2.42
0.25	21.98	56.83	6.17
0.30	34.60	64.28	8.99
0.35	46.28	71.05	10.56
	(47.42)	(72.55)	(10.69)
0.40	54.87	76.19	11.51
0.46	60.29	79.74	12.06
	(61.86)	(81.77)	(12.21)

J_1	J_2	J_3	J_4	J_5	J_6
0.216	0.111	0.066	−0.123	0.046	−0.039

ted as a function of the energy for $T=1.10T_C^{\text{calc}}$ and various ζ values. The curves for $\zeta=0.35$ and 0.46 have pronounced maxima at ± 8.0 and ± 9.3 mev, respectively, beside the maximum at zero energy, while the curve for $\zeta=0.25$ exhibits a small shoulder only at about ± 6 meV, and the curve for $\zeta=0.15$ is similar to a Lorentzian. In general, $F_{\text{TP}}(q,\omega)$ develops a side peak, if $\delta_2<2\delta_1$. For comparing the theory with the experiment, the paramagnetic scattering was calculated using Eq. (1) with Eq. (2) as spectral weight function and convoluted with the experimental resolution by numerical integration. The values for the inverse correlation length κ_1 were taken from Ref. 11. κ_1 is about 0.08 Å^{-1} for $1.10T_C$. The resulting theoretical curves are shown in Figs. 2 and 3 as dashed lines. An individual scale factor was the only free parameter used for fitting these curves to the measured profiles. The comparison with the experiment demonstrates, that the energy widths of the calculated curves are in reasonable agreement with the observed widths, not, however, the pronounced side peaks predicted for the large-q values. This characteristic feature of the calculated curves is not reflected by the data, in contrast to EuO, where peaks at finite energy are observed for large-q values, which are well described by the three-pole approximation theory.

The reasons for the discrepancy between predicted and measured line shapes in Pd_2MnSn are not clear. The fits are not improved, if the usual approximation for τ given by Eq. (3) is relaxed, treating τ as a free parameter, while keeping δ_1 and δ_2 fixed at the calculated values. The fits converge at almost the same values of τ as derived from Eq. (3). Good agreement with the experiment, however, is obtained, if δ_1 and δ_2 are free to vary, while τ is given by Eq. (3). Fits with such a parametrized three-pole approximation theory are shown as solid lines in Figs. 2 and 3, and the values obtained for δ_1 and δ_2 are listed in Table II. While the fitted δ_1 values are similar to the theoretical values, δ_2 differs up to a factor of 2 from the theory. Since the energy widths are not very sensitive to δ_2, the theoretical linewidths and the linewidths derived from the parametrized curves are in reasonable agreement. This is demonstrated by Fig. 5, where the solid curve represents the HWHM values (Γ values) calculated for $T=1.10T_C^{\text{calc}}$ from δ_1 and δ_2 as listed in Table I, while the symbols denote the HWHM values derived from the fitted δ_1 and δ_2 values of Table II. The difference between the calculation for $1.10T_C^{\text{calc}}$ and $1.09T_C^{\text{calc}}$ is negligible, as far as the spectral shape and the linewidth are concerned. The parametrized three-pole approximation curve follows the experimental data so closely, much better than a Lorentzian or a Gaussian, that it seems to be justified to use it as a model function for deconvoluting the measured profiles. The Γ values derived from these curves and

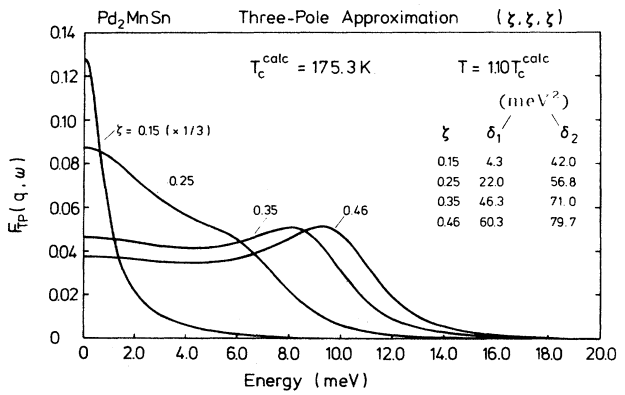

FIG. 4. Theoretical curves, calculated by the three-pole approximation theory for the [111] direction in Pd_2MnSn at $T=1.10T_C^{\text{calc}}$. The spectral weight function $F_{\text{TP}}(q,\omega)$ is plotted as a function of the energy for $\zeta=0.15$, 0.25, 0.35, and 0.46. Note, that the curve for $\zeta=0.15$ is scaled by the factor $\frac{1}{3}$. The theoretical δ_1 and δ_2 values used for calculating the curves are given in the figure.

TABLE II. δ_1, δ_2, and Γ values obtained from the fits with the parametrized three-pole approximation theory to the measurements with unpolarized and polarized neutrons, respectively. The estimated standard deviations are given in parentheses.

	Unpolarized beam setup (20'-20'-20'-40')			Polarized beam setup (40'-80'-80'-130')		
ζ	δ_1 (meV)^2	δ_2 (meV)^2	Γ (meV)	δ_1 (meV)^2	δ_2 (meV)^2	Γ (meV)
0.10				1.1(0.4)	15.1(10.6)	0.4(1.0)
0.15	3.6(0.2)	16.4(2.4)	1.3(0.4)			
0.25				26.5(2.7)	93.5(18.2)	4.5(2.7)
0.35	52.9(1.2)	156.4(7.2)	8.0(0.9)	45.9(6.4)	120.3(34.0)	8.8(2.4)
0.46	68.8(1.8)	169.9(9.6)	11.4(0.8)	64.4(15.5)	187.1(79.5)	9.0(4.9)

plotted as symbols in Fig. 5 may thus be interpreted as resolution corrected observed HWHM values.

In spite of the good agreement between the parametrized three-pole approximation theory and the experimental data, it is not clear, whether the small shoulder exhibited at higher-q values is really manifest in the data. From a direct inspection of the measured profiles one gains the impression, that a singly peaked function with the maximum at zero energy and without any additional structure should also be able to describe the data within the experimental statistics. It is well known, that in the small-q regime and at temperatures close to T_C asymptotic renormalization-group theory[3,4] should be valid, except for the very small-q values, $q < q_d$, where dipolar interactions become important.[7,8] For Pd_2MnSn the dipolar wave vector q_d can be calculated to be 0.01 Å^{-1} from κ_1 and the susceptibility measurements reported in Ref. 17. Such small-q values were not studied in the present experiments. The spectral weight function based on the asymptotic renormalization-group theory is given by

$$F_R(q,\omega)=\frac{1}{\pi}\frac{1}{Aq^{2.5}}\mathrm{Re}\left[\frac{1}{is+\alpha(1+is\beta/\alpha)^{-0.6}}\right], \quad (4)$$

where $\alpha=0.78$, $\beta=0.46$, and $s=\omega/Aq^{2.5}$, which is equivalent to $s=\omega/\Gamma$. For Pd_2MnSn the diffusion constant A is 60 meV Å$^{2.5}$ (Ref. 11). If one assumes, that A is experimentally known, Eq. (4) has no free parameters. The dashed curve in Fig. 5 represents the ζ dependence of Γ according to the dynamical scaling. It can be seen, that the deconvoluted experimental values start to deviate from this curve at $\zeta\approx0.15$, and tend to saturate, when approaching the zone boundary at $\zeta=0.5$. In Ref. 11 this "bending over" of Γ as a function of ζ was successfully approximated by the heuristic function

$$\Gamma(\zeta)=\Lambda^*(1-\cos2\pi\zeta), \quad (5)$$

with $\Lambda^*=4.06$ meV at $T=210$ K and q in [111] direction. The Γ values had been derived by fitting the data with a pure Lorentzian as spectral weight function. At the higher-q values, the fits with a Lorentzian, however, are significantly worse than the fits with the parametrized three-pole approximation theory. Looking for a better fitting, singly peaked, spectral weight function, we found it tempting, therefore, to test the validity of a parametrized $F_R(q,\omega)$ function for describing the paramagnetic scattering over a wide q range. For this purpose Eq. (5) was modified in such a way, that $\Gamma(\zeta)$ was effectively used as a free parameter, replacing the dynamical scaling expression $Aq^{2.5}$ by

$$\Gamma(\zeta)=\tilde{\Lambda}2\sin^z(\pi\zeta). \quad (6)$$

For $z=2$ Eq. (6) is identical to Eq. (5); for $z=2.5$ and

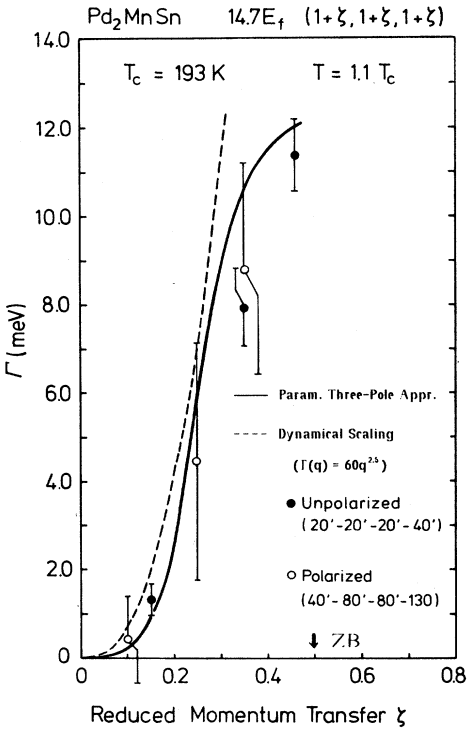

FIG. 5. Observed and calculated Γ values as a function of ζ. The open and solid dots denote Γ values derived from the fits with the parametrized three-pole approximation theory to the measurements with the polarized and unpolarized beam setup, respectively. They can be regarded as resolution deconvoluted observed HWHM values. The data from the polarized measurements have rather large errors due to the limited counting rate. The solid line represents the calculation based on the three-pole approximation theory without adjustable parameters. The dashed line shows the ζ dependence of Γ as predicted by the dynamical scaling expression $\Gamma=Aq^{2.5}$ with $A=60$ meV Å$^{2.5}$ from Ref. 11.

small arguments $\pi\xi$ Eq. (6) corresponds to the dynamical scaling. This modified spectral weight function should thus be able to interpolate smoothly between the correct theoretical approach of the asymptotic renormalization-group theory at small-q values and the heuristic description of the observed "bending over" of the linewidths at large-q values. In the final fits with this modified function, shown as dot-dashed lines in Figs. 2 and 3, z was kept fixed at a medium value $z=2.2$, while $\tilde{\Lambda}$ and a scale factor were the only free parameters. $\tilde{\Lambda}$ converged at 4.92(6) meV. It can be seen from Figs. 2 and 3, that the fits with this type of a singly peaked, but otherwise featureless, spectral weight function are less satisfactory than the fits with the parametrized three-pole approximation theory. They are, however, significantly better than fits with a Lorentzian.

IV. CONCLUSIONS

The present work is focused on the paramagnetic scattering at large-q values, where a thorough physical understanding has not yet been gained. It was found, that the measured profiles can well be described by applying the three-pole approximation theory with δ_1 and δ_2 as adjustable parameters. On the other hand, these parameters can be calculated from known magnetic exchange constants making the three-pole approximation a parameter-free theory. The theoretical linewidths thus obtained are in reasonable agreement with the measured linewidths, not, however, the details of the calculated line shapes. The pronounced side peaks predicted by the theory are not reflected by the data. The reasons for this failure of the theory are not clear. The discrepancy cannot be overcome by abandoning the approximation for τ given by Eq. (3). The development of the side peaks in the theoretical curves is also not very sensitive to modifications of the exchange constants J_i or the value S of the spin. For example, making $|J_4|$ 20% smaller has almost no influence on the side peaks, though it would change T_C^{calc} to 192 K in good agreement with the observed T_C. It is also not expected, therefore, that using more than six exchange constants, as suggested by Ref. 1, will lead to essentially different theoretical profiles. Attempts with a singly peaked, but otherwise featureless, spectral weight function derived from the renormalization-group theory also did not lead to a better description of the measured profiles, than was obtained by the parametrized three-pole approximation theory.

The present measurements seem to confirm the conjecture expressed in Ref. 15: in contrast to the short-ranged magnetic system EuO, where peaks at finite energy occur at large q, which are well described by the three-pole approximation theory, the long-ranged magnetic system Pd_2MnSn does not show any excitations above T_C, not even at the zone boundary (in recently published measurements on Ni,[18] however, peaks at very high energies were found, which are claimed to represent spin-wave-like excitations). A satisfactory theoretical description of the line shapes at large-q values is still lacking. Theoretical approaches based on the mode-coupling theory will perhaps give new insight.

ACKNOWLEDGMENTS

We are grateful to Y. Yamaguchi and the late Y. Ishikawa for many stimulating discussions. One of us (H.G.) would like to express thanks for the kind hospitality of the members of the neutron scattering group during his stay at Brookhaven. This work was carried out as a part of the U.S.-Japan collaboration on neutron scattering. Work at Brookhaven supported by the Division of Materials Sciences, U.S. Department of Energy under Contract No. DE-AC02-76CH00016.

*Formerly at Brookhaven National Laboratory, Upton, New York 11973.
†Permanent address: Paul Scherrer Institut, 5232 Villigen PSI, Switzerland.

[1]Y. Noda and Y. Ishikawa, J. Phys. Soc. Jpn. **40**, 690 (1976).
[2]Y. Noda and Y. Ishikawa, J. Phys. Soc. Jpn. **40**, 699 (1976).
[3]R. Folk and H. Iro, Phys. Rev. B **32**, 1880 (1985).
[4]R. Folk and H. Iro, Phys. Rev. B **34**, 6571 (1986).
[5]G. Shirane, P. Böni, and J. L. Martinez, Phys. Rev. B **36**, 881 (1987).
[6]P. Böni, M. E. Chen, and G. Shirane, Phys. Rev. B **35**, 8449 (1987).
[7]F. Mezei, J. Magn. Magn. Mater. **45**, 67 (1984).
[8]F. Mezei, B. Farago, S. M. Hayden, and W. G. Stirling, Physica B **156-157**, 226 (1989).
[9]E. Frey, F. Schwabl, and S. Thoma, Phys. Lett. A **129**, 343 (1988).
[10]E. Frey and F. Schwabl, Z. Phys. B **71**, 355 (1988).
[11]G. Shirane, Y. J. Uemura, J. P. Wicksted, Y. Endoh, and Y. Ishikawa, Phys. Rev. B **31**, 1227 (1985).
[12]M. Kohgi, Y. Endoh, Y. Ishikawa, H. Yoshizawa, and G. Shirane, Phys. Rev. B **34**, 1762 (1986).
[13]S. W. Lovesey and R. A. Meserve, J. Phys. C **6**, 79 (1973).
[14]A. P. Young and B. S. Shastry, J. Phys. C **15**, 4547 (1982).
[15]P. Böni and G. Shirane, Phys. Rev. B **33**, 3012 (1986).
[16]R. A. Cowley, G. Shirane, R. J. Birgeneau, and H. J. Guggenheim, Phys. Rev. B **15**, 4292 (1977).
[17]K. R. A. Ziebeck, P. J. Webster, P. J. Brown, and J. A. C. Bland, J. Magn. Magn. Mater. **24**, 258 (1981).
[18]H. A. Mook, D. Mck. Paul, and S. Hayden, Phys. Rev. B **38**, 12 058 (1988).